Differences in cortical activation during smooth pursuit and saccadic eye movements following cerebellar lesions

Baumann, O; Ziemus, B; Luerding, R; Schuierer, G; Bogdahn, U; Greenlee, M W

Published in:
Experimental Brain Research

DOI:
10.1007/s00221-007-0922-3

Differences in cortical activation during smooth pursuit and saccadic eye movements following cerebellar lesions

O. Baumann[1,3], B. Ziemus[2,4], R. Luerding[2], G. Schuierer[5], U. Bogdahn[2] & M.W Greenlee[1]

1. Department of Experimental Psychology, University of Regensburg, Universitätsstrasse 31, 93053, Regensburg, Germany
2. Department of Neurology, University of Regensburg, Regensburg, Germany
3. Department of Psychology, University of Oslo, Oslo, Norway
4. Clinical Neurophysiology, University of Maastricht, Maastricht, The Netherlands
5. Department of Neuroradiology, University of Regensburg, Regensburg, Germany

Correspondence to M. W. Greenlee.

This is a post-peer-review, pre-copyedit version of an article published in Experimental Brain Research.

The final authenticated version is available online at: http://dx.doi.org/10.1007/s00221-007-0922-3

Abstract

Current evidence supports the proposal that the cerebellum mediates the activity of other brain areas involved in the control of eye movements. Most of the evidence so far has concentrated on the vermis and flocculi as the cerebellar agents of oculomotor control. But there is also evidence for an involvement of the cerebellar hemispheres in eye movement control. Straube et al. (Ann Neurol 42:891–898, 1997) showed that lateral hemispheric lesions affect initiation of smooth pursuit (SPEM) and saccadic eye movements. Ron and Robinson (J Neurophysiol 36:1004–1022, 1973) evoked smooth pursuit and saccadic eye movements by electrical stimulation of crus I and II, as well as in the dentate nuclei of the monkey. Functional MRI studies also provide evidence that the cerebellar hemispheres play a significant role in SPEM and saccadic eye movements. To clarify the role of the cerebral hemispheres in eye movement control we compared the eye movement related blood oxygen level dependent (BOLD) responses of 12 patients with cerebellar lesions due to stroke with those of an aged-matched healthy control group. Six patients showed oculomotor abnormalities such as dysmetric saccades or saccadic SPEM during the experiment. The paradigm consisted of alternating blocks of fixation, visually guided saccades and visually guided SPEM. A nonparametric random-effects group analysis showed a degraded pattern of activation in the patient group during the performance of SPEM and saccadic eye movements in posterior parietal areas putatively containing the parietal eye fields.

Introduction

More than a century ago Hitzig (1874) and Ferrier (1874) conducted studies to investigate the contribution of the cerebellum in the control of eye movements. In the more recent past studies using functional magnetic resonance imaging (fMRI) as well as electrophysiological and anatomical tracer studies provided new evidence about the cortical and subcortical cerebellar circuits that control eye movements. A large literature exists regarding disturbances of eye movements following lesions in the cerebellum (Optican and Robinson 1980; Lewis and Zee 1993; Robinson, Straube and Fuchs 1993; Raymond, Lisberger and Mauk 1996; Versino, Hurko and Zee 1996). In most studies the flocculi and the vermis were identified as the responsible structure for the control of eye movements. The neocerebellum, also referred to as the cerebellar hemispheres, was traditionally thought to be only involved in the control of coordinated movements and the maintenance of the muscle tonus (Luciani 1891; Glickstein 2006). In the mean time mounting evidence indicates that also the hemispheres of the cerebellum are involved in the control of eye movements. Ron and Robinson (1973) evoked smooth pursuit and saccadic eye movements by electrical stimulation of crus I and II, as well as the dentate nuclei in monkey. In addition, Straube, Scheuerer and Eggert (1997) showed that patients with isolated lesions in hemispheres of the cerebellum exhibited an impaired ability to execute eye movements. Neuroimaging methods (fMRI and positron emission tomography, PET) supplied further evidence by showing an increased blood oxygen level dependent (BOLD) signal in the neocerebellum during the

This is a post-peer-review, pre-copyedit version of an article published in Experimental Brain Research.

The final authenticated version is available online at: http://dx.doi.org/10.1007/s00221-007-0922-3

execution of both smooth pursuit eye movements (SPEM) and saccades (Dieterich, Bucher, Seelos and Brandt 2000; Tanabe et al. 2002).

In order to further elucidate the role of the neocerebellum in the control of eye movements, fMRI was conducted in patients with isolated lesions (resulting from stroke of the posterior inferior and/or superior cerebellar arteries) in the lateral zone of the cerebellum while they executed SPEM and saccades. In order to detect abnormalities in brain activity, an age and gender matched control group of 12 healthy volunteers was also examined. We hypothesize that the cerebellar patients exhibit abnormal cerebral neural activity pattern during the execution of eye movements. Compensatory augmentation or reductions in activity in those brain regions that are relevant for the control of eye movement would indicate a role of the cerebellum in oculomotor control. On the cortical level these regions-of-interest (ROI) would be the frontal (FEF), supplementary (SEF) and parietal eye fields (PEF), the cingulate gyrus, the areas MT and MST and the precuneus; on subcortical level the lateral geniculate nucleus (LGN) and the basal ganglia (Krauzlis and Stone 1999; Krauzlis 2005; Lynch and Tian 2005) could be involved. The FEF, SEF, PEF, precuneus/cuneus as well as the middle temporal area (MT) and the medial superior temporal area (MST) are all reciprocally connected, receive direct input from the visual association cortex and have direct projections to the oculomotor neurons in the brain stem (Lynch and Tian 2005). Eye movements can be elicited or modified by electrical stimulation in all these areas, and lesions in these areas lead to impairments in saccadic as well as in smooth pursuit eye movements. However if only one of these areas is damaged eye movement control is only partially impaired (Lynch and Tian 2005). The thalamus, superior colliculus (SC), the basal ganglia and the cerebellum are connected in feedback loops with the cerebral centres and exhibit a modulatory influence (Lynch and Tian 2005).

Following cerebellar damage, augmented activity in one of these brain areas would indicate a compensatory recruitment. On the other hand, decreased brain activity in eye movement control centres could be interpreted as a direct consequence of damaged cerebellar–cortical projections. The statistical comparison of the activity patterns of the patient and of the controls group could thereby reveal insight to the functional cross-linking of the neocerebellum with other brain regions that are involved in the control of eye movements.

Methods

The study was approved by the local ethics committee. Written informed consent was obtained from all participants.

Subjects

Twelve patients with isolated cerebellar infarctions (eight men, four women: mean age 49 years, standard error (SE) = 3.3 years; range 35–69 years.) were recruited from the Neurology Department of the University Hospital of Regensburg. All patients fulfilled the inclusion criteria of isolated stroke in neocerebellum detected by MRI. Infarct size and location were determined on the basis of T2- and T1- weighted images by a neuroradiologist.

We included patients in an acute phase of stroke (2–8 days past infarction), as well as patients in a post-acute phase (2 months past infarction) or in a chronic phase (up to 6 years after cerebellar infarction).

A control group consisted of twelve healthy controls matched for age and sex for each patient (mean age 46 SD = 3.2; range 35–68 years) (see Fig. 1 for T1-weighted images of infarcted region of the cerebellum and Table 1 for further patient characteristics).

Fig. 1

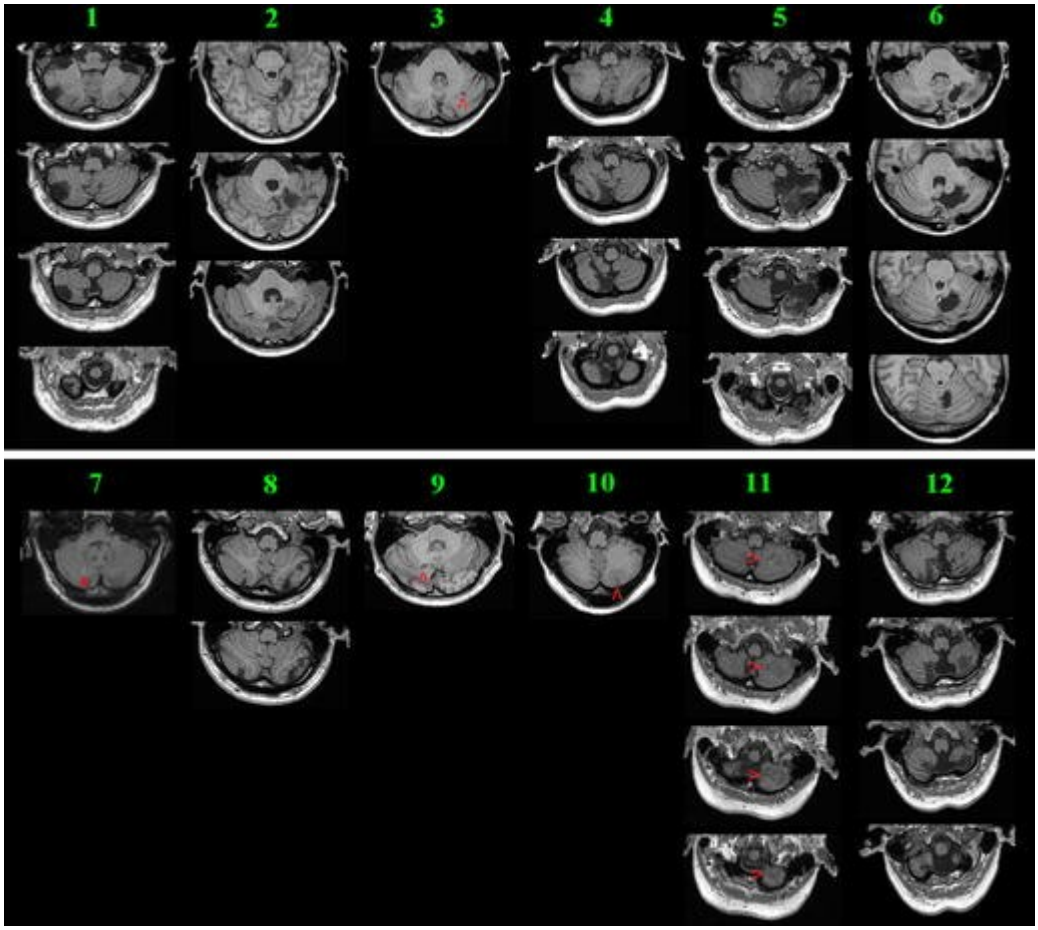

Axial structural T1-weighted MRI scans at the level of maximum infarct volume for each patient performed at the time of the fMRI. An expert neuroradiologist documented the location and extent of each lesion by comparing these to T2-weighted images. In cases where the lesion is small or of low contrast, a red arrow indicates the lesion location within the imaged section

Table 1 Overview of patient characteristics

Patient	Age	Sex	Infarct age	Infarct localization	Size cm	Oculomotor deficit
1	63	M	5 yrs	Left PICA	3 × 3 × 3 (l)	Dysmetric saccades
2	39	M	4 yrs	Right SCA	1.5 × 2 × 1.5 (r)	Mildly saccadic SPEM
3	38	F	18 m	Right SCA	0.3 × 0.3 × 0.3 (r)	–
4	43	F	6 yrs	Left PICA	3 × 2 × 0.5 (l)	–
5	48	M	3 yrs	Right PICA	4 × 2 × 5 (r)	–
6	53	F	2 m	Right PICA	3 × 4 × 3.5 (r)	Saccadic SPEM
7	48	M	2 d	Left PICA	0.5 × 0.3 × 0.5 (l) 0.5 × 0.5 × 0.5 (l)	Dysmetric saccades
8	42	M	14 m	Right PICA Left SCA	2 × 2 × (r) 0.5 × 0.4 × 0.5 (l)	–
9	41	M	2 m	Left PICA	1 × 1 × 1 (l) 0.5 × 0.4 × 0.5 (l)	Dysmetric saccades
10	34	F	2.5 m	Right PICA	5 × 2 × 5 (r)	–
11	68	M	14 d	Right PICA	3 × 3 × 2 (r)	Severely saccadic SPEM
12	65	M	0.5 m	Right PICA Left PICA	2 × 2 × 1 (r) 2 × 2 × 1 (l)	–

The average pairwise age difference between the respective members of the patient and control groups was 3 years (range 0–5 years). All study subjects were right handed according to the Edinburgh Handedness Inventory. Exclusion criteria were the use of psychotropic medication, vascular damage in other brain regions or a history of former strokes, cognitive impairment due to dementia, history of neurological and/or psychiatric illness (other than cerebellar disease), claustrophobia, pregnancy and the presence of ferromagnetic surgical pins. All subjects in the control and the patients groups had normal vision, and any refractive corrections ranged within ± 1.5 dioptres. All subjects were made familiar with the task before the experiment, by demonstrating to them the stimuli and task outside of the scanner on a separate monitor.

Infarcts were either located in the right, the left or both hemispheres of the cerebellum (right-hemisphere = 5, left-hemisphere = 3, both hemispheres = 4). The size of the lesion varied considerably. A subdivision according to the size of the lesion could not be made due to the small number of subjects. All relevant parameters of the group of patients are specified in Table 1.

Paradigm

The subjects were positioned supine in the scanner with their head tightly secured in the headcoil to minimize head movement. They viewed the stimuli with a mirror that reflected the image from the projection screen placed at the head of the subject in the end of the scanner gantry. The stimuli were digital movies created with Matlab (Version 6.5). The subjects had to accomplish three different tasks during an fMRI session: execution of SPEM, execution of saccades and as a baseline a third task, in which the subjects had only to fixate a central target. The visual target was in all three conditions a small red square (0.4° visual angle (0.4°, 13 cd/m2)) on black background (1.25 cd/m2). In the condition with SPEM the target moved with a sinusoidal velocity profile along the horizontal axis starting from the centre; at completion of a whole cycle the dot changed its direction of motion. The left and right turning points were at 24° visual angle from each other. The maximum speed of 15.1°/s was reached by the dot in the screen centre. A full cycle lasted 5 s and a block contained altogether four entire cycles. An experimental block had therefore a duration of 20 s (see Fig. 2a). In the condition with the visually guided saccades the target moved with the same temporal pattern like in the SPEM condition, only that the dot jumped every 1250 ms, starting in the centre, with steps of 12° visual angle to the left and right. An experimental block with saccadic eye movements lasted also 20 s (see Fig. 2b). The fixation condition also had a duration of 20 s. In Fig. 2c the pattern is shown, according to which the conditions fixation, saccades and SPEM alternated over time. The whole experiment had accordingly a duration of only 3 min, due to the fact that the patients should not be strained too much. This task was embedded in a working memory task and the entire scan period including anatomical T1-weighted images lasted approximately 20 min.

Fig. 2

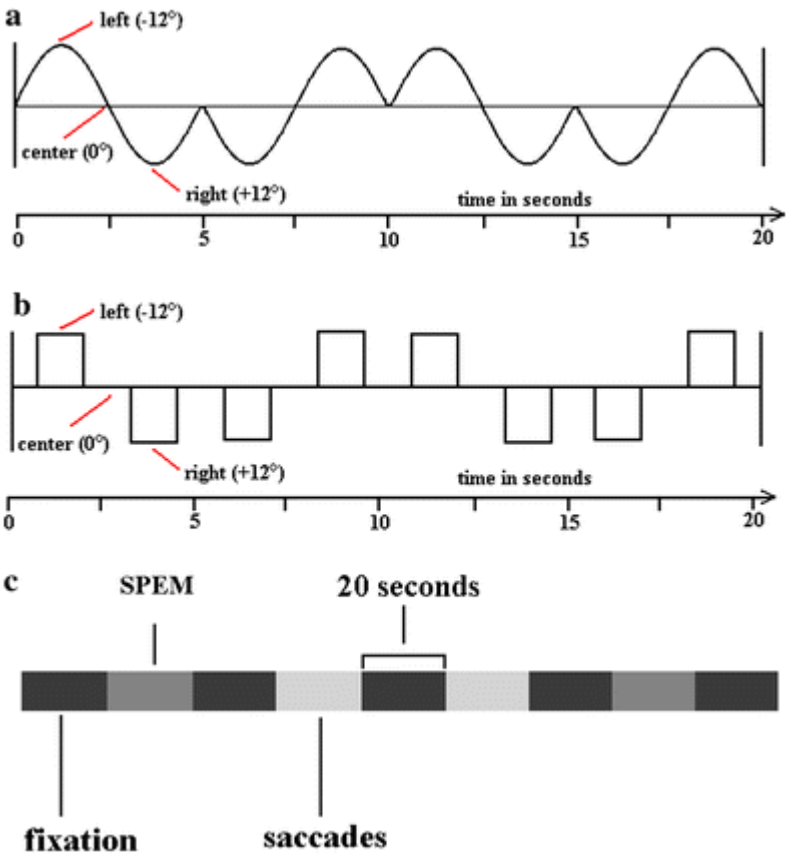

a Time course of on experimental block of the SPEM task. **b** Time course of one experimental block of the saccadic task. **c** Temporal order of the three conditions in the experiment (SPEM, saccades, fixation)

MRI-imaging

The functional scans were acquired on a 1.5 Tesla Siemens Magnetom (Sonata, Siemens, Erlangen, Germany) equipped with a fast gradient system (40 mT/m with slew rate of 200 T/M/s) for echo-planar (EPI) imaging and a 8-channel phase array full-head radio-frequency (RF) receive-transmit headcoil (MR-Devices). Functional imaging was performed using a T2*-weighted gradient echo planar imaging (EPI) covering the whole brain. We acquired volumes with 34 axial slices with a gap of 0.3 mm and could thus image the entire brain. The field of view (FOV) measured 192 mm with a voxel matrix size 64 × 64, resulting in a voxel size of 3 × 3 × 3 mm. The TR was 3000 ms. The time to echo corresponded to TE = 50 ms, the flip angle corresponded to 90°. The first two EPI images were discarded as “dummy” images before the start of the experimental paradigm in order to obtain steady-state. After the functional runs, anatomical high resolution sagittal T1-weighted images were acquired with the MP-Rage sequence (magnetization prepared, rapid acquisition gradient echo). The cerebellum was excluded from the functional acquisition to prevent artefact due to the stroke lesions in the patient group.

FMRI data analysis

Data were processed and analyzed on a single-subject level using Statistical Parametric Mapping SPM 2 (SPM2, Wellcome Department of Cognitive Neurology, London, UK; http://www.fil.ion./ucl.ac.uk/spm/) implemented in MATLAB (The MathWorks Inc.). Echo planar images were unwarped and realigned to the first acquired volume to correct for head movement.

The images were then transformed into a standard stereotaxic anatomical space (Talairach and Tournoux 1998; Friston 1995a). We used the following procedure to normalize the scans: A T2*-weighted mean image of the unsmoothed images was co-registered with the corresponding anatomical T1-weighted image of the same individual. The individual T1-image was used to derive the transformation parameters for the stereotaxic fit using the MNI-Template (Friston et al. 1995a), which was then applied to the individual single coregistered EPI images. Functional images were smoothed with a 3D-Gaussian kernel (full width, half maximum, FWHM = 12 mm).

Analysis using the General Linear Model (GLM) (Friston et al. 1995b) was done after applying high-pass filtering (cut-off: 128 s). The periods in which subjects performed the task were modelled separately for the SPEM and the saccades condition by using a temporal rectangular function (boxcar) convolved with the homodynamic response function. The fixation condition served as a baseline. On group level we conducted a random-effects analysis, using the non-parametric SnPM-Toolbox (Holmes 1994; Holmes et al. 1996) with a statistical threshold of P = 0.05 (Tmax contrast analysis, corrected for multiple comparisons). Montreal Neurological Institute (MNI) coordinates were transformed to Talairach coordinates by using the WFU-Pickatlas (Wake Forest University Pickatlas, Version 1.02, Maldjian et al. 2003). The anatomical locations were identified by using the program MNI Space Utility (MSU) by S. Pakhomov. This tool relies on the mni2tal program combined with data of the Talairach demon (Lancaster et al. 1997, 2000).

Recording and analysis of eye movements

During the fMRI measurement, eye movements were recorded to monitor task performance. Eye movements were recorded using the MR-Eyetracker (Cambridge Research Systems, Ltd), a fiber-optic limbus tracking device (Kimmig et al. 1999). The Matlab Data Acquisition Toolbox was used to acquire the signals derived from the MR-Eyetracker. The sampling frequency of the eye-tracker signal was 500 Hz, the best spatial resolution was 0.1°. The eye-recording system was calibrated with four eccentricities (−10°, −5°, +5°, +10°), to determine the deviation from the fixation position. Using the Matlab Signal Processing Toolbox, we analyzed the eye trajectories offline and evaluated the task performance of the subjects.

About half of the patients exhibited disturbances of eye movements during the experiment, which were characterized by dysmetric saccades or saccadic pursuit. Apart from that all subjects were able to follow the instructions, and they were able to maintain central fixation (no saccadic or pursuit intrusions) and to follow the target dot with SPEM or saccades, respectively. For the conditions with saccadic eye movements and SPEM the response times were measured from the onset of target movement to the beginning of the eye movement.

The evaluation of the response times were conducted, due to the relatively small data set, manually with the Matlab Toolbox SPTool.

Results

Oculomotor data

Exemplary data for the saccadic and pursuit tasks are presented in Fig. 3a–c. The mean onset latency of a saccade corresponded to 286 ms (SE 96 ms) for the patients and to 174 ms (SE 20 ms) for the control group. For the SPEM the mean onset latency was 163 ms (SE 30 ms) for the patients and 109 ms (SE 10 ms) for controls. Wilcoxon tests indicated that the onset times of the saccades and the SPEM differed significantly from each other. This was true for both the control group ($P < 0.05$) and at the patient group ($P < 0.01$). The onset times of the controls and the patients were also compared, separately for SPEM and saccades, with Mann-Whitney U tests. The differences between the two groups were, however, neither significant for saccades ($P = 0.20$) nor SPEM ($P = 0.74$). This may be attributed to the large variance of the response times in the group of patients and to the relatively small sample size.

Fig. 3

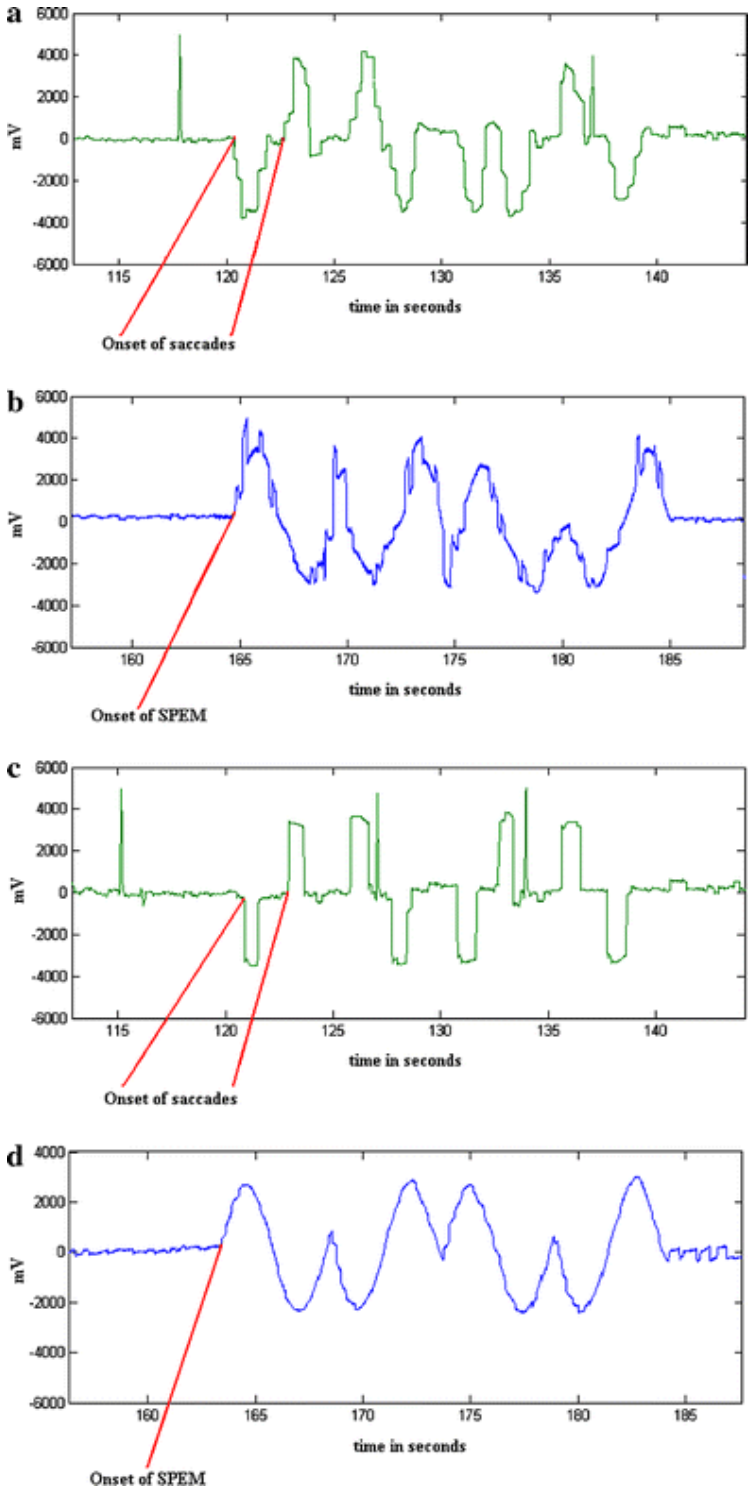

a Eye movements (eye position in millivolts) of a patient during execution of saccades. **b** Eye movements of a patient during execution of SPEM **c** Eye movements of a healthy control subject during execution of saccades. **d** Eye movements of a healthy control subject during execution of SPEM

Functional MRI data

The following comparisons show the differences of the neural activity during the execution of SPEM and saccades in relation to central fixation. The test for more pronounced BOLD signal in the fixation condition than in the conditions with eye movements led to no significant result. The comparisons are represented first for the control group and then for the patients. Finally the activation patterns of the control and the patient groups are compared.

Cortical activations during eye movements: control group

SPEM > fixation

In the statistical analysis this comparison led to a total of five activated clusters. The largest activation extended bilaterally with 23,633 voxels from the cuneus and precuneus to the inferior occipital gyrus (IOG), middle occipital gyrus (MOG) and superior occipital gyrus (SOG), the lingual gyrus, the inferior parietal lobule (IPL), superior parietal lobule (SPL) as well as exclusively right-hemispheric activation in the superior temporal gyrus (STG) and to the supramarginal gyrus (SMG) (Brodmann areas 7, 18, 19, 31, 37, 39 and 40). The second largest cluster with 2281 voxels extended over the right superior frontal gyrus (SFG), middle frontal gyrus (MFG) and the precentral gyrus as well as the left SFG, MFG, inferior frontal gyrus (IFG) and Precentral gyrus (Brodmann areas 4 and 6). The IFG was activated on the right side in the form of a separate medium-sized cluster (163 voxels, Brodmann area 6). The third biggest cluster (803 voxels) extended over the left SPL Brodmann (area 7). See Fig. 4a and Table 2.

Fig. 4

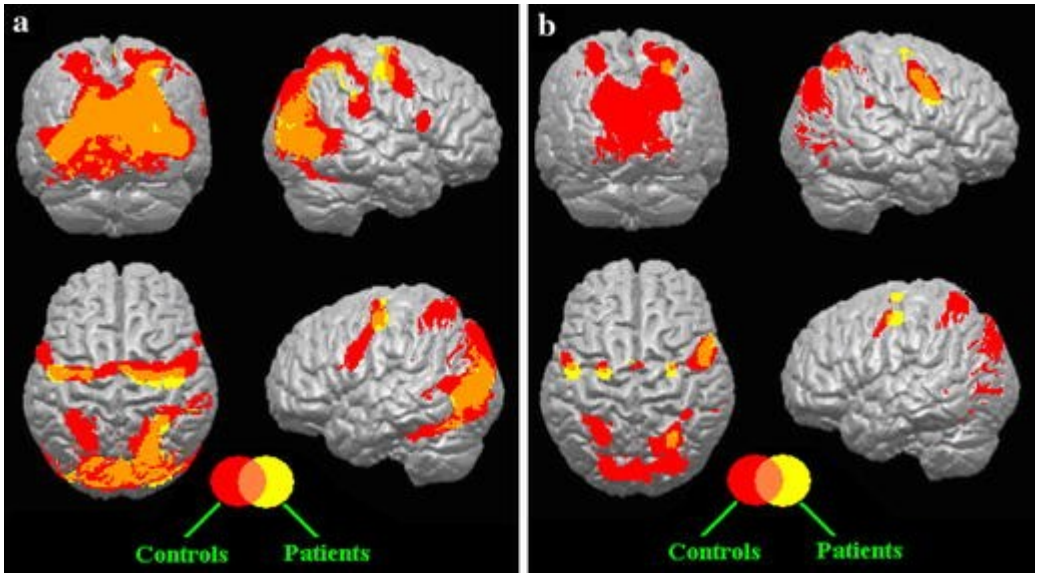

a Group activation maps of controls (*red*) and patients (*yellow*) for the contrast "SPEM > Fixation". **b** Group activation maps of controls (*red*) and patients (*yellow*) for the contrast "Saccades > Fixation". Overlaps are indicated by intermediate colors (see color inset). Activation is shown overlaid onto a rendered MNI-normalized template (activated voxels deep in sulci are projected onto the surface). Significant voxels surpassing a threshold of $P = 0.05$ (corrected for multiple comparisons) are presented

Table 2 Pseudo-*t*-values and Talairach coordinates of activation maxima for the contrasts "SPEM > Fixation", "Saccades > Fixation" and "SPEM > Saccades" in healthy controls ($P < 0.05$, corrected for multiple comparisons)

Region	Hemisphere	Brodmann area	Talairach coordinates			(pseudo)-t-values of maxima (clustersize in number of voxels)
			x	*y*	*z*	
Controls: SPEM > Fixation						
MTG/SMG/LG/SOG MOG/IOG/Cun/Prec/SPL/ IPL/SMG	R + L	7/18/19/31/37/ 39/40	0	−81	15	15.69 (23633)
SFG/MFG/IFG/PreCeG	R + L	4/6	26	−7	50	6.75 (2281)
SPL	L	7	−28	−48	52	6.87 (803)
IFG	R	6	55	14	14	5.55 (163)
SMG	R	40	50	−44	19	4.72 (3)
Controls: Saccades > Fixation						
Cun/Prec/LG/SOG/IPL/ SPL	R + L	7/18/19/31	10	−77	13	10.78 (7856)
SFG/MFG/PreCeG	R	4/6	52	6	38	7.72 (680)
SPL	R	7	26	−61	62	7.50 (597)
SPL	L	7	−26	−54	52	6.40 (496)
PreCeG/SFG	L	6	−51	−3	50	5.24 (72)
IPS	R	40	38	−46	48	5.12 (52)
MFG	L	6	−26	−7	50	5.29 (45)

Region	Hemisphere	Brodmann area	Talairach coordinates			(pseudo)-t-values of maxima (clustersize in number of voxels)
			x	*y*	*z*	
SMG	**R**	**40**	**61**	**−37**	**30**	**5.29 (30)**
MFG	**R**	**6**	**26**	**−7**	**48**	**5.02 (16)**
SFG	**R + L**	**6**	**0**	**−5**	**61**	**4.83 (11)**
Controls: SPEM > Saccades						
Cun/Prec/LG/SOG/MOG/ IOG	**R + L**	**7/18/19/31**	**14**	**−85**	**19**	**7.56 (2514)**
MOG/MTG	**R**	**37**	**52**	**−68**	**3**	**7.86 (569)**
PoCeG/SMG	**R**	**2/40**	**61**	**−24**	**34**	**8.37 (478)**
STG/SMG	**L**	**22/40**	**−65**	**−13**	**8**	**5.96 (233)**
PreCeG	**L**	**4**	**−61**	**−10**	**28**	**6.44 (122)**
MOG	**L**	**19**	**−52**	**−69**	**9**	**6.24 (76)**
SPL	**R**	**7**	**16**	**−48**	**58**	**6.31 (70)**
Prec	**R**	**19**	**16**	**−80**	**39**	**5.52 (21)**

For each cluster the hemisphere, Brodmann areas and anatomical structures are specified, in which the respective cluster is located. *Cun* cuneus, *IFG* inferior frontal gyrus, *IOG* inferior occipital gyrus, *IPL* inferior parietal lobule, *IPS* intraparietal sulcus, *L* left, *LG* lingual Gyrus, *MFG* middle frontal gyrus, *MOG* middle occipital gyrus, *MTG* middle temporal gyrus, *PoCeG* postcentral gyrus, *Prec* precuneus, *PreCeG* Precentral Gyrus; *R* right, *SFG* superior frontal gyrus; *SMG* supramarginal gyrus, *SOG* superior occipital gyrus, *SPL* superior parietal lobule, *STG* superior temporal gyrus

Saccades > fixation

This comparison led to ten significant BOLD clusters. The largest encompassed the cuneus, precuneus, lingual gyrus, the superior occipital gyrus (SOG), the intraparietal lobule (IPL) and extended in particular in the right hemisphere up to the inferior border of the superior parietal lobule (SPL; Brodmann areas 7, 18, 19, 31). A separate significantly activated cluster was present in the SPL bilaterally (right with a size of 579 and left with a size of 496 voxels). The superior frontal gyrus (SFG), the middle frontal gyrus (MFG) and the precentral gyrus (Brodmann area 6) were also bilaterally activated. In the right hemisphere we observed a large cluster (680 voxels) and in the left hemisphere two smaller BOLD clusters (72 and 45 voxels). Furthermore a right hemispheric cluster was evident within the intraparietal sulcus (IPS) (52 voxels, Brodmann area 40) and another in the supramarginal gyrus (SMG; 30 voxels, Brodmann area 40). A small bilateral activation (11 voxels) in the medial part of the SFG (area 6), which corresponds the supplementary eye field (SEF) (see Fig. 4 b and Table 2), was evident.

Contrast: SPEM > saccades

In the direct statistical comparison of the activity patterns of SPEM and saccades the cuneus, precuneus, the lingual gyrus as well as the inferior, medial and superior occipital gyri (IOG, MOG, SOG) and middle temporal gyrus (MTG) (including MT) (Brodmann areas 7, 18, 19 and 31, 37) were bilaterally more activated in the SPEM condition. Furthermore a right hemispheric cluster, in the area of the SMG and the postcentral gyrus (478 voxels, Brodmann areas 2 and 40, and a left hemispheric analogue, which were somewhat more inferior within the region of SMG and STG (233 voxels, Brodmann areas 22 and 40) were present. Finally there was an exclusively right hemispheric activation in the SPL (70 voxels, Brodmann area 7).

Contrast: Saccades > SPEM

In the direct statistical contrast there was no significantly more pronounced activity for the saccades condition compared to the SPEM condition.

Cortical activations during eye movements: patients group

Contrast: SPEM > fixation

The statistical analysis of this comparison led to altogether six activated clusters. The largest activation extended bilaterally (8544 voxels) from the cuneus and precuneus to the inferior, medial and superior occipital gyri, the lingual gyrus, the IPL and the SPL (Brodmann areas 7, 18, 19 and 31). The second largest cluster of 611 voxels extended over the right SFG, MFG and the precentral gyrus (Brodmann areas 4 and 6) and the third largest with 273 voxels over the left SFG, MFG and precentral gyrus (Brodmann areas 4 and 6). Furthermore there were three small to medium sized left hemispheric clusters in the putamen, the MOG and in the right SMG (see Fig. 4 a and Table 3).

Table 3 Pseudo-*t*-values and talairach coordinates of activation maxima for the contrasts "SPEM > Fixation", "Saccades > Fixation" and "SPEM > Saccades" in patients ($P < 0.05$, corrected for multiple comparisons)

Region	Hemisphere	Brodmann area	Talairach coordinates			(pseudo)-*t*-values of maxima (clustersize in number of voxels)
			x	*y*	*z*	
Patients: SPEM > Fixation						
LG/SOG/MOG/IOG/Cun/Prec/ SPL/IPL	R + L	7/18/19/31	−36	−81	4	8.83 (8544)
SFG/MFG/PreCeG	R	4/6	36	−15	45	6.67 (611)
SFG/MFG/PreCeG	L	4/6	−48	−9	50	6.37 (273)
Putamen	L	–	−24	−11	6	5.71 (53)
SMG	R	40	54	−37	35	5.20 (23)
MOG	L	19	−20	−86	−8	5.15 (19)
Patients: Saccades > Fixation						
SFG/MFG/IFG/PreCeG	R	4/6	52	0	44	5.78 (274)
SFG/MFG/PreCeG	L	4/6	−50	−11	49	6.37 (91)
SPL	R	7	26	−66	54	6.06 (49)
MFG	R	6	26	−9	61	5.28 (42)
PreCeG	L	6	−26	−10	63	5.43 (42)
SFG	L	6	−6	−3	57	5.01 (4)
Patients: SPEM > Saccades						

Region	Hemisphere	Brodmann area	Talairach coordinates			(pseudo)-*t*-values of maxima (clustersize in number of voxels)
			x	*y*	*z*	
Cun/Prec	R + L	18/19/31	4	−86	34	6.38 (186)
MOG/IOG/MTG	L	19/37	−42	−80	−6	5.71 (102)
MOG	R	19	34	−83	4	5.69 (29)
Prec	R + L	31	2	−65	18	5.41 (15)
MTG	R	37	48	−70	2	5.45 (12)

For each cluster the hemisphere, Brodmann areas and anatomical structures are specified, in which the respective cluster is located. For abbreviations Table 2

Contrast: Saccades > fixation

This comparison led to six significant BOLD clusters. The largest was in the right hemisphere in the region of the precentral gyrus, SFG, MFG and IFG (Brodmann areas 4 and 6) (total, 274 voxels). In the left hemisphere there were similar activations, however limited to the precentral gyrus, SFG and MFG (Brodmann areas 4 and 6) (91 and 42 voxels). Exclusively the right SPL was activated (49 voxels). Another spatially limited activation was detected in the left hemisphere (4 voxels) in the medial part of the SFG, which corresponds to the SEF (see Fig. 4 b and Table 3).

Contrast: SPEM > saccades

In the direct statistical comparison of the BOLD signal from SPEM and saccades, altogether five clusters were found to be activated. The largest cluster with 186 voxels extended bilaterally over cuneus and precuneus (area 18, 19 and 31). The second largest cluster (102 voxels) were situated in the left-hemisphere and extended over the IOG, MOG and MTG (Brodmann areas 19 and 37). In the right hemisphere a similar pattern with a cluster in the MOG (29 voxels, Brodmann area 19) and in the MTG (12 voxels, Brodmann area 37) was evident. The activations in the temporal cortex included area MT bilaterally.

Contrast: Saccades > SPEM

In the direct statistical comparison to the SPEM condition there was no significantly more pronounced activity in the saccades condition.

Differences between patients and controls

In the patient group no brain regions were additionally or significantly more strongly activated than in the control group. To the contrary, the control group exhibited significantly more pronounced activation compared to the patient group.

SPEM (SPEM > fixation): control group > patient group

For the comparison of the two groups we found on cluster level (with a „cluster-defining"-threshold of $t = 2$ and a level of significance of $\alpha = 0.05$ corrected for multiple comparisons) a significant difference. As illustrated in Fig. 5 a, b, compared to the patients the controls showed a more pronounced activation in the cuneus and the lingual gyrus (Talairach coordinates $x = 6$, $y = -83$, $z = 13$; pseudo-t-value = 4.27; 5715 voxels, Brodmann areas 7, 18, 19, 23 and 31) during the execution of SPEM. However, in a descriptive comparison of the two groups also differences in the activity patterns can be observed in the FEF as well as in the posterior parietal cortex (including IPS and SMG) (see Fig. 4 a).

Fig. 5

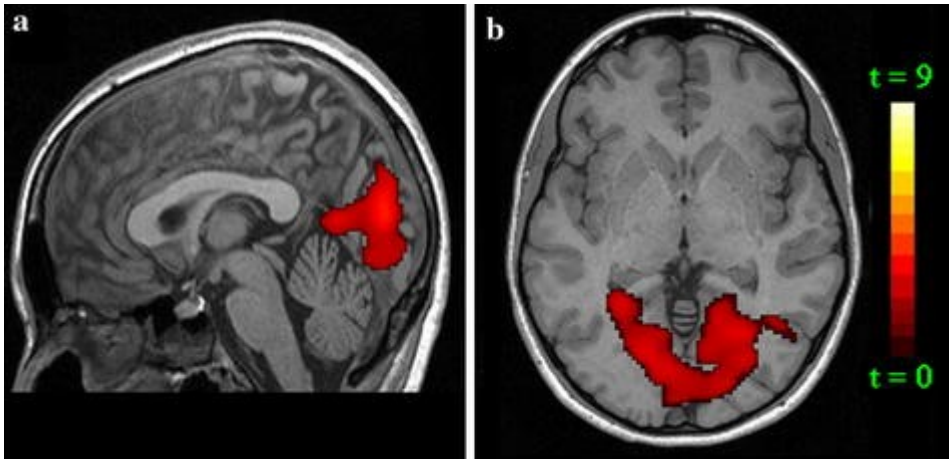

Group activation maps illustrating the contrasts between controls and patients (SPEM > fixation in controls > SPEM > fixation in patients). Significant clusters surpassing a threshold of $P = 0.05$ (corrected for multiple comparisons, cluster-defining threshold $t = 2.0$) are presented. **a** Pseudo-t values are overlaid onto a saggital slice of an MNI-normalized template. **b** Pseudo-t values are overlaid onto an axial slice of an MNI-normalized template

Saccades (saccades > fixation): control group > patient group

In the direct statistical comparison there was no significantly more pronounced activity for the controls compared to the patients during the execution of saccades. However in a

descriptive comparison the healthy controls revealed stronger activity in the cuneus, the FEF as well as in the posterior parietal cortex (SPL, IPL and SMG) (see Fig. 4 b).

ROI analysis of the cuneus

A region of interest (ROI) analysis was conducted for the cuneus using "Marsbar" (Brett, Anton, Valabregue and Poline 2002). The BOLD signal of the voxels in the cuneus was averaged and the relative change of the BOLD signal during the SPEM and the saccade condition was computed in comparison to the average activity in this ROI for the entire fMRI measurement. The percent change of the BOLD signal was determined first for each test subject separately and afterwards the mean values and standard errors were calculated for each group and each condition. The cuneus was defined as a spherical volume with a radius of 15 mm, whose centre is located at the Talairach coordinates $x = 0$, $y = -71$, $z = 11$. This ROI corresponds to the brain area, in which the controls exhibited a more pronounced activation in the contrast „SPEM > Fixation" compared to the patients (see Fig. 5 a, b). This ROI analysis revealed that the patients exhibited a BOLD signal change in the cuneus that was about half the size of the response in the controls during the execution of SPEM and saccades. However, only for the SPEM condition did the difference between patients and controls reach statistical significance (*U*-test, $P \leq 0.05$). Both the control and patient group clearly exhibit greater changes of signal during the SPEM than during the saccade condition. The standard errors were of similar size for both groups and for both conditions (see Fig. 6). This difference in the effect of cerebellar lesions on activation in the cuneus suggests that this area is more involved in smooth pursuit than it is in saccades.

Fig. 6

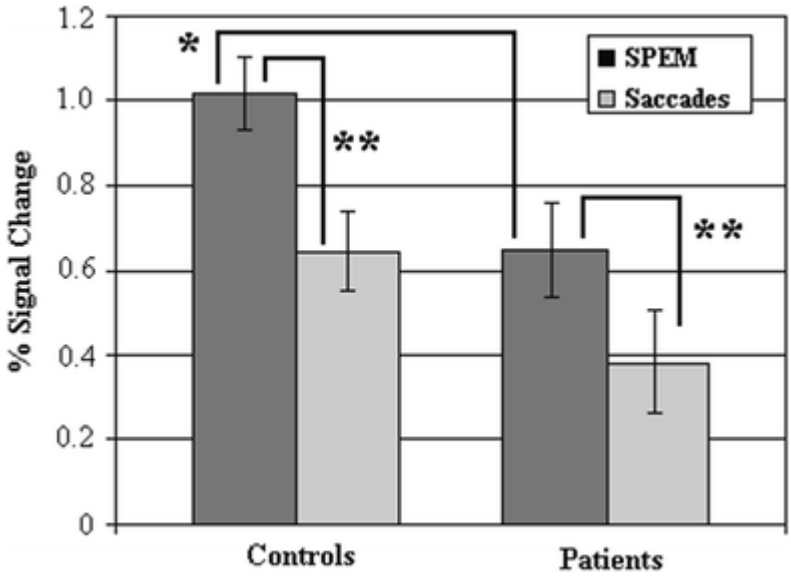

Percent BOLD-signal change averaged separately over the control and patient group for the „SPEM" and the „Saccades" condition (*Error bars* = ±1SE); * Significant, $P \leq 0.05$; ** Highly significant, $P \leq 0.01$; (Wilcoxon-Test for within-group analysis/*U*-test for between-group analysis)

Discussion

In order to further elucidate the role of the neocerebellum in the control of eye movements, we investigated the pattern of BOLD activation during the execution of SPEM and saccades in patients with isolated lesions in the lateral zone of the cerebellum. The comparison of the results to those of a group of healthy controls showed that in the patients some brain regions were less activated during the oculomotor tasks than that found for the control group. Since we monitored eye movements during fMRI we could rule out a possible role of saccadic or pursuit intrusions during the fixation condition and non-compliance to the task, as a possible explanation for the weak BOLD signals in the patient group.

During the execution of SPEM and saccades the control group showed activations in brain regions known to be eye movement centres (Leigh and Zee 2006; Tanabe et al. 2002; Lynch and Tian 2005). As such the FEF, the posterior parietal cortex (PPC) (including the IPS), the MT/MST area and the cuneus/precuneus were active. To a certain degree also striate and extrastriate parts of the visual cortex were active (V1 peripheral as well as V2). The largest differences between SPEM and saccades in the healthy controls were evident in significantly more pronounced activations in the region MT and in the cuneus during the execution of SPEM. These findings correspond to those of earlier studies (Kimmig et al. 1999; Petit and Haxby 1999). The finding of Berman et al. (1999) that saccades lead to spatially more extended BOLD clusters in the FEF than SPEM could not be replicated in our study. In our study the SPEM condition resulted in spatially more extended BOLD clusters than the condition with saccades. However, several differences in the experimental designs, like the predictability of the targets, prevent a direct comparison of the results.

In patients well-established eye movement centres were active during the execution of SPEM. As such the FEF, the PPC (including the IPS) as well as cuneus and precuneus were active. During the execution of saccades only the FEF and the PPC were found to be active. The cuneus and precuneus as well as the visual cortex were not significantly activated.

In the direct statistical comparison the patient group showed a significant lower activation in the cuneus than the controls during the execution of SPEM. In a ROI analysis of the cuneus the BOLD signal changes were compared directly during the different experimental conditions. The activity differences in the cuneus cannot be simply explained by more variance of the BOLD signal in the patient group. As it can be seen in Fig. 6 the standard errors of the BOLD signal changes of the patient and controls were highly similar.

In a descriptive comparison of the results from the patient and the control group (see Fig. 4a, b) the cuneus, the FEF, the PPC and precuneus showed an attenuated activation pattern for the patients during the execution of SPEM and saccades. As mentioned above, the cortical and subcortical networks for eye movement control are complex and not yet completely investigated. The finding that the cuneus, the precuneus, the FEF and the PPC showed an attenuated activation pattern due to damage in the neocerebellum is an interesting result. However, a statistical assessment of the relationship between quantitative measures of eye movement deficits (e.g. number of saccadic intrusion during SPEM, deviation

of saccades from the saccadic target) and BOLD signal in these regions could not be conducted due to the small number of patients with the same type of oculomotor abnormality.

Cuneus and precuneus are already well-known for their role in the execution of SPEM and saccades, visual motion perception and in attentional control. Recent neuroimaging studies showed that during both SPEM and saccades activation in the precuneus and cuneus can be observed (Law et al. 1997; Petit et al. 1999; O' Driscoll et al. 2000). In monkeys the area 7 m corresponds to the cuneus and the area DM (Cavada and Goldman Rakic 1989) corresponds to the precuneus (Tian and Lynch 1996). Both regions are thought to be forwarding visual motion information to the FEF and receiving projections via thalamus from the cerebellum. In addition, there are projections from the precuneus via the pons to the cerebellum (Tian and Lynch 1996), and the area DM receives signals from MT, MST and FEF (Stanton et al. 1995; O' Driscoll et al. 2000). In a recent study investigating the connectivity of the cerebellum Allen et al. (2005) could show that projections between the dentate nuclei (located in the lateral cerebellar hemispheres) to the precuneus/cuneus (as well as further cortical regions) exist. In this context the result of an fMRI study of Vanni et al. (2001) is likewise interesting, who found that in humans the cuneus receives information from primary visual areas, modifying it and forwarding it to higher visual areas. In the light of our result, namely that in the patient group the BOLD signal was reduced compared to that shown by the controls, we conclude that the lateral cerebellum participates in the control of eye movements and projects particularly to the precuneus and cuneus.

Conclusion

Our results show that lesions limited to the cerebellar hemispheres lead to pronounced alterations in the neural activity in cortical areas that are involved in the control of eye movements (like the FEF, the IPS and the cuneus). This finding corroborates the role of the neocerebellum in the control of eye movements. The results suggest in particular a strong functional coupling of the neocerebellum with the medial parieto-occipital cortex (cuneus/precuneus). Since both the cerebellum and the medial parieto-occipital cortex are also known to participate in the perception of visual motion we suggest that both structures play an important role in the control of smooth pursuit and in the perception of visual motion during ocular pursuit.

References

Allen G, McColl R, Barnard H, Ringe WK, Fleckenstein J, Cullum CM (2005) Magnetic resonance imaging of cerebellar-prefrontal and cerebellar-parietal functional connectivity. Neuroimage 28:39–48

Berman RA, Colby CL, Genovese CR, Voyvodic JT, Luna B, Thulborn KR, Sweeney JA (1999) Cortical networks subserving pursuit and saccadic eye movements in humans: an FMRI study. Hum Brain Mapp 8:209–225

Brett M, Anton JL, Valabregue R, Poline JP (2002) Region of interest analysis using an SPM toolbox. Neuroimage 16:497

Cavada C, Goldman-Rakic PS (1989) Posterior parietal cortex in rhesus monkey: I. Parcellation of areas based on distinctive limbic and sensory corticocortical connections. J Comp Neurol 287:393–421

Dieterich M, Bucher SF, Seelos KC, Brandt T (2000) Cerebellar activation during optokinetic stimulation and saccades. Neurology 54:148–155

Ferrier D (1874) The location of function in the brain. Proc R Soc Lond B Biol Sci 22:229

Friston KJ, Ashburner J, Poline JP, Frith CD, Heather JD, Frackowiak RSJ (1995a) Spatial registration and normalization of images. Hum Brain Mapp 2:165–189

Friston KJ, Holmes AP, Worseley KJ, Poline JP, Frith CD, Frackowiak RSJ (1995b) Statistical parametric maps in functional imaging: a general linear approach. Hum Brain Mapp 2:189–210

Glickstein M (2006) Thinking about the cerebellum. Brain 129:288–290

Hitzig E (1874) Physiologische und klinische Untersuchungen über das Gehirn. Gesammelte Abhandlungen. Part I. Berlin: Hirschwald

Holmes AP (1994) Statistical issues in functional brain mapping. [Doctoral Dissertation], University of Glasgow

Holmes AP, Blair RC, Watson JDG, Ford I (1996) Non-parametric analysis of statistic images from functional mapping experiments. J Cereb Blood Flow Metab 16:7–22

Kimmig H, Greenlee MW, Huethe F, Mergner T (1999) MR-Eyetracker: a new method for eye movement recording in functional resonance imaging. Exp Brain Res 126:443–449

Krauzlis RJ (2005) The control of voluntary eye movements: new perspectives. Neuroscientist. 11(2):124–137

Krauzlis RJ, Stone LS (1999) Tracking with the mind's eye. Trends Neurosci 22:544–550

Lancaster JL, Summerlin JL, Rainey L, Freitas CS, Fox PT (1997) The talairach daemon, a database server for talairach atlas labels. Neuroimage 5:633

Lancaster JL, Woldorff MG, Parsons LM, Liotti M, Freitas CS, Rainey L, Kochunov PV, Nickerson D, Mikiten SA, Fox PT (2000) Automated talairach atlas labels for functional brain mapping. Hum Brain Mapp 10:120–131

Law I, Svarer C, Hom S, Paulsen OB (1997) The activation pattern in normal humans during supression, imagination and performance of saccadic eye movements. Acta Physiol Scand 161:419–434

Leigh RJ, Zee DS (2006) The neurology of eye movements, 4th edn. Oxford University Press, New York

Lewis RF, Zee DS (1993) Ocular motor disorders associated with cerebellar lesions: pathophysiology and topical localization. Rev Neurol (Paris) 149:665–677

Luciani L (1891) II cerveletto: nouvi studi di fisiologia normale e patologica. Firenze: Le Monnier

Lynch JC, Tian JR (2005) Cortico-cortical networks and cortico-subcortical loops for the higher control of eye movements. Prog Brain Res 151:461–501

Maldjian JA, Laurienti PJ, Kraft RA, Burdette JH (2003) An automated method for neuroanatomic and cytoarchitectonic atlas-based interrogation of fMRI data sets. Neuroimage 19:1233–1239

O'Driscoll GA, Wolff AL, Benkelfat C, Florencio PS, Lal S, Evans AC (2000) Functional neuroanatomy of smooth pursuit and predictive saccades. Neuroreport 11:1335–1340

Optican LM, Robinson DA (1980) Cerebellar-dependent adaptive control of primate saccadic system. J Neurophysiol 44:1058–1076

Petit L, Haxby JV (1999) Functional anatomy of pursuit eye movements in humans as revealed by fMRI. J Neurophysiol 82:463–471

Raymond JL, Lisberger SG, Mauk MD (1996) The cerebellum: a neuronal learning machine? Science 272:1126–1131

Robinson FR, Straube A, Fuchs AF (1993) Role of the caudal fastigial nucleus in saccade generation. II. Effects of muscimol inactivation. J Neurophysiol 70:1741–1758

Ron S, Robinson DA (1973) Eye movements evoked by cerebellar stimulation in the alert monkey. J Neurophysiol 36:1004–1022

Stanton GB, Bruce CJ, Goldberg ME (1995) Topography of projections to posterior cortical areas from the macaque frontal eye fields. J Comp Neurol 353:291–305

Straube A, Scheuerer W, Eggert T (1997) Unilateral cerebellar lesions affect initiation of ipsilateral smooth pursuit eye movements in humans. Annals of Neurology 42:891–898

Talairach J, Tournoux P (1988) Co-Planar stereotaxic atlas of the human brain. Stuttgart: Thieme

Tanabe J, Tregellas J, Miller D, Ross RG, Freedman R (2002) Brain activation during smooth-pursuit eye movements. Neuroimage 17:1315–1324

Tian JR, Lynch JC (1996) Corticocortical input to the smooth and saccadic eye movement subregions of the frontal eye field in cebus monkeys. J Neurophysiol 76:2754–2771

Versino M, Hurko O, Zee DS (1996) Disorders of binocular control of eye movements in patients with cerebellar dysfunction. Brain 119:1933–1950

Vanni S, Tanskanen T, Seppa M, Uutela K, Hari R (2001) Coinciding early activation of the human primary visual cortex and anteromedial cuneus. Proc Natl Acad Sci USA 98:2776–2780